

Modeling Uranium Transport in Koongarra, Australia: The Effect of a Moving Weathering Zone¹

Anton Leijnse,^{2,3} Hendrika van de Weerd,^{2,4}
and S. Majid Hassanizadeh^{2,5}

Natural analogues are an important source of long-term data and may be viewed as naturally occurring experiments that often include processes, phenomena, and scenarios that are important to nuclear waste disposal safety assessment studies. The Koongarra uranium deposit in the Alligator Rivers region of Australia is one of the best-studied natural analogue sites. The deposit has been subjected to chemical weathering over several million years, during which many climatological, hydrological, and geological changes have taken place, resulting in the mobilization and spreading of uranium. Secondary uranium mineralization and dispersed uranium are present from the surface down to the base of the weathering zone, some 25 m deep. In this work, a simple uranium transport model is presented and sensitivity analyses are conducted for key model parameters. Analyses of field and laboratory data show that three layers can be distinguished in the Koongarra area: (1) a top layer that is fully weathered, (2) an intermediate layer that is partially weathered (the weathering zone), and (3) a lower layer that is unweathered. The weathering zone has been moving downward as the weathering process proceeds. Groundwater velocities are found to be largest in the weathering zone. Transport of uranium is believed to take place primarily in this zone. It appears that changes in the direction of groundwater flow have not had a significant effect on the uranium dispersion pattern. The solid-phase uranium data show that the uranium concentration does not significantly change with depth within the fully weathered zone. This implies that uranium transport has stopped in these layers. A two-dimensional vertically integrated model for transport of uranium in the weathering zone has been developed. Simulations with a velocity field constant in time and space have been carried out, taking into account the downward movement of this zone and the dissolution of uranium in the orebody. The latter has been modelled by a nonequilibrium relationship. In these simulations, pseudo-steady state uranium distributions are computed. The main conclusion drawn from this study is that the movement of the weathering zone and the nonequilibrium dissolution of uranium in the orebody play an important role in the transport of uranium. Despite the fact that the model is a gross simplification of what has actually happened in the

¹Received 12 March 1999; accepted 7 December 1999.

²National Institute of Public Health and the Environment (RIVM), P. O. Box 1, 3720 BA Bilthoven, The Netherlands.

³Department of Environmental Sciences, Subdepartment of Water Resources, Wageningen Agricultural University, Nieuwe Kanaal 11, 6709 PA Wageningen, The Netherlands. e-mail: a.leijnse@rivm.nl

⁴Present address: Department of Environmental Sciences, Subdepartment of Soil Science and Plant Nutrition, Wageningen Agricultural university, P. O. Box 8005, 6700 EC Wageningen, The Netherlands.

⁵Present address: Department of Water Management, Sanitary and Environmental Engineering, Delft University of Technology, P. O. Box 5048, 2600 GA Delft, The Netherlands.

past two million years, a reasonable fit of calculated and observed uranium distributions was obtained with acceptable values for the model parameters.

KEY WORDS: radionuclides, natural analogue, transport modeling, Alligator River.

INTRODUCTION

In safety assessment studies of the disposal of radioactive waste in geological formations, simulation of radionuclide transport by groundwater plays a central role. In the event of escape of contaminants from a deep geological repository, the most probable mechanism for release of radionuclides to the biosphere is transport of species via groundwater (International Atomic Energy Agency, 1981). Simulation of nuclide transport in groundwater is achieved by means of mathematical models that describe various migration and reaction processes. Such models must be evaluated in terms of the validity and reliability of their predictions. However, given the very long lifetime required for repositories and the time scale of various processes, an evaluation of the validity of models employed in safety assessment studies cannot be achieved by conventional methods. Natural analogue studies may provide a valuable alternative in this regard.

Natural analogues are an important sources of long-term data and may be viewed as naturally occurring experiments that often include processes, phenomena, and scenarios that are important to safety assessment studies. Migration and retardation of radionuclides are observed in natural geological systems over distances of meters to hundreds of meters and time scales of thousands to millions of years.

One of the best-studied natural analogue sites is the Koongarra site in the Alligator Rivers Region of the Northern Territory in Australia (Fig. 1). Uranium orebodies in this area and the weathering and transport processes are believed to provide an appropriate natural analogue for the migration of a series of radionuclides through the geosphere. Executive field studies for characterization of the Koongarra site have been carried out since 1981 (Snelling, 1992), initially to investigate the economic potential of the site, and later as part of the Alligator Rivers Analogue Project (ARAP). The experimental and modeling project ARAP was set up in 1987 under the auspices of the Organisation for Economic Co-operation and Development (OECD) Nuclear Energy Agency (NEA) with the Australian Nuclear Science and Technology Organisation (ANSTO) as project manager. Main objectives of the ARAP project have been to understand: (1) processes that have contributed significantly to the formation of the present day uranium ore deposit, (2) weathering of the Koongarra region, and (3) alteration of the host rock and primary uranium. Field studies have been supplemented with modeling efforts directed at studying groundwater flow, migration pathways, rock/water interactions, uranium transport, and formation and continued alteration of secondary mineralization (Duerden, 1992).

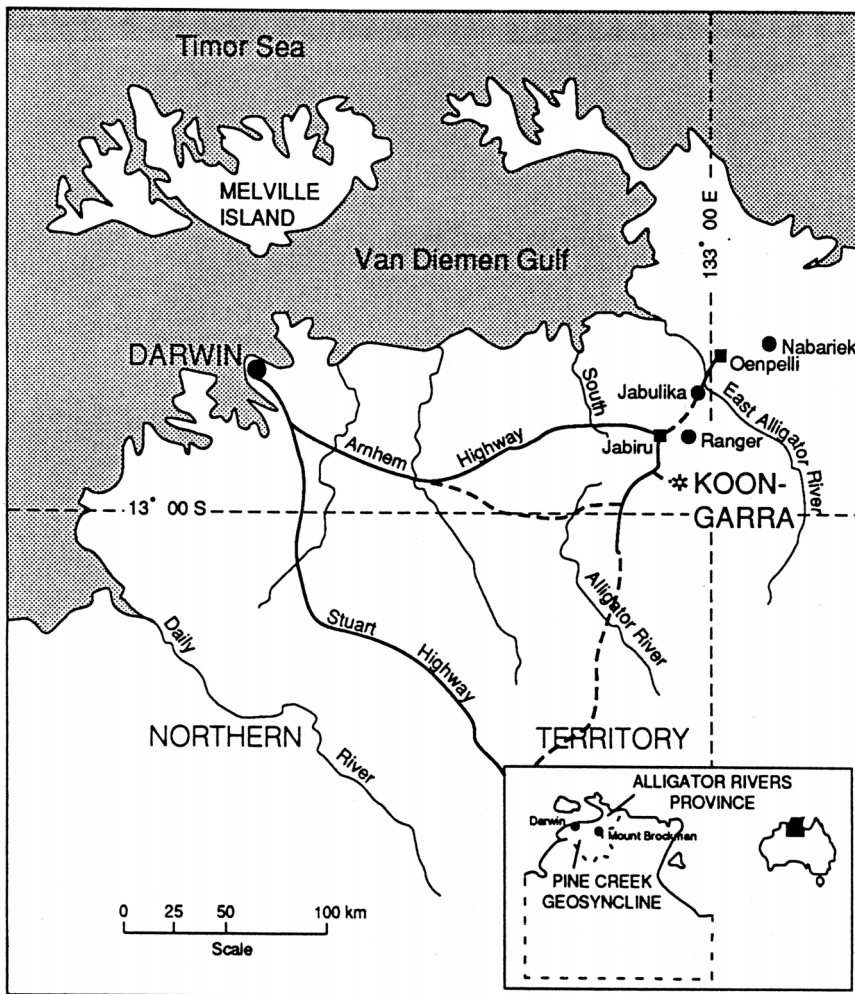


Figure 1. Koongarra, Alligator Rivers Region.

The data set of Alligator Rivers Natural Analogue Project has been made available to modelers in a number of international modeling studies, among them the INTRAVAL study (Duerden, 1992). In this work, results of the modeling of the transport of uranium in the weathering zone of the Koongarra site, carried out in the framework of INTRAVAL, are presented and discussed.

In the next section, a brief description of the geology and the hydrological characteristics of Koongarra is given. Next, the uranium distribution is analyzed. The mass balance equation describing transport of uranium at Koongarra and

parameter values used in the numerical simulations of transport are given. Results of the numerical simulations are discussed and, finally, conclusions are presented.

HYDROGEOLOGICAL CHARACTERISTICS OF THE KOONGARRA SITE

The Koongarra ore zone has been the subject of extensive exploration studies. A number of geological, hydrogeological, geochemical, and topographical surveys have been carried out over the years. Results of these studies have appeared in ARAP Progress Reports, and in the ARAP Final Reports (OECD/NEA, 1994). A geomorphological study was carried out to obtain a general idea of the history of the site (Wyrwoll, 1992). Hydrogeological data have been obtained from a series of drawdown and recovery tests, water pressure tests, aquifer tests, and slug tests (Davis, Marley, and Norris, 1992). To define geohydrological parameters and to discriminate between various units, a number of petrophysical measurements were carried out on core samples originating from different zones in the study area. Additionally, a geoelectrical measurement program was carried out in order to characterize the subsurface of the Koongarra site and to determine the extent of potentially conductive fracture zones (Emerson and others, 1992). In this section, a very brief description of hydrogeological characteristics of the site is given, based on the work of Snelling (1992).

Local geology is dominated by the Cahill and Kombolgie Formations. The Cahill Formation consists of two members. The lower member consists mainly of a thick basal dolomite and the upper member of a sequence of chloritized quartz-mica schists. The Cahill Formation consisted originally of shale, sandstone, and limestone that were deposited about 2200 million years ago. These rocks were subsequently metamorphosed to schist and dolomite between 1870 and 1800 million years ago. Sandstone layers of the Kombolgie Formation were deposited on top of the Cahill Formation between 1690 and 1600 million years ago. At the Koongarra site, however, movement of rocks along the Koongarra Reverse Fault uplifted and tilted the layers, causing a local reversal of this normal sequence. Subsequent weathering and erosion have removed the sandstone overlying the uplifted schist so that now the schist layers are exposed to the processes of weathering and erosion. The zone of contact between the schist and the sandstone is delineated by the reverse fault (Fig. 2).

The schist layers of Cahill Formation host a natural uranium mineralization that formed between 1600 and 1550 million years ago. Two distinct but clearly related orebodies, separated by about 100 m of barren schists, have been identified. Both bodies consist of primary zones containing uraninite veins within a zone of steeply dipping, sheared quartz-chlorite schists of the lower member of the Cahill Formation. The more southwesterly of the two orebodies, the No. 1 orebody,

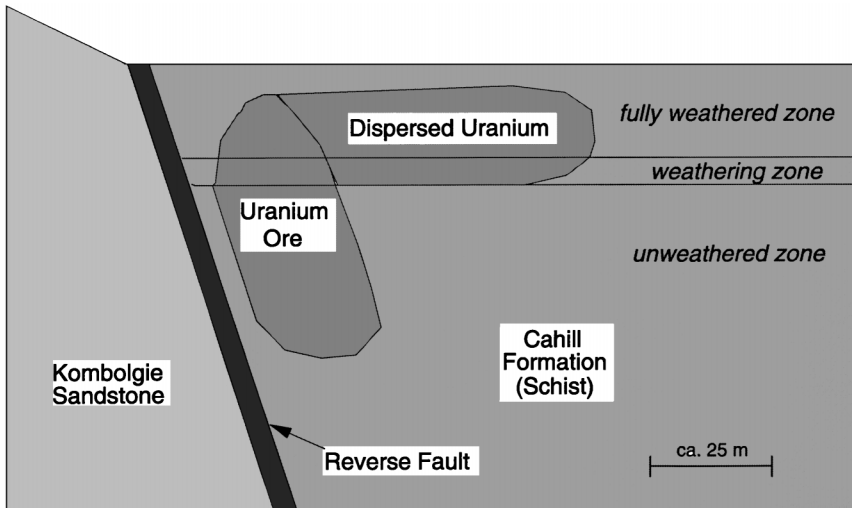


Figure 2. Schematic north-south cross section of the Koongarra site; representation of the three layers representing different stages of weathering.

is elongated over a distance of 450 m and persists to a depth of about 100 m. This orebody is located next to the Koongarra Reverse Fault, and as a result of weathering and erosion now lies near the ground surface (Fig. 2). The No. 1 orebody has been the subject of study in the ARAP test case of INTRAVAL and the study reported here.

Weathering processes alter the hydrogeological properties of the schist. In the early stages of weathering, fractures, and fissures existing in the unweathered schists are widened, resulting in a significant increase in permeability. During later stages, however, the formation of excess clay minerals has caused these fissures and fractures to be blocked, and this in turn has resulted in a major reduction of permeability of the rock (Emerson and others, 1992). Presently, one can identify three distinct layers in the Cahill schist (Fig. 2):

1. A fully weathered top layer with a thickness of about 20 m. This layer has an average permeability of about 1.1 md and an average porosity of around 0.34. Very little groundwater flow takes place in this layer.
2. An partially weathered intermediate layer with a thickness of about 5 m. This zone has a rather high permeability with the average value varying from 35 to 60 md. The vertical permeability is about two times smaller than the horizontal permeability. Average porosity is about 0.12–0.16. The upper and lower boundaries of this zone move downward as the weathering

process continues: more clay is formed at the top and the fissures and fractures are widened at the bottom. The groundwater flow is thought to occur mainly through the microfractured matrix (Emerson and others, 1992). We refer to this zone as the “weathering zone.”

3. An unweathered lower zone that has a very low matrix permeability (less than 1 md). The unweathered rock is quite tight with a porosity less than 0.02. Fracture flow, however, is evident from aquifer tests reported by Davis, Marley, and Norris (1992).

One of the most important features of the uranium mineralization at Koongarra is the occurrence of abundant secondary uranium minerals, principally within the dispersion fan above the No. 1 orebody. Secondary uranium mineralization and dispersed uranium derived from decomposition and leaching of the primary mineralized zone are present from the surface down to the base of weathering, some 25 m deep. These form an elongated body of ore grade material dispersed down slope for about 80 m to the southeast (Fig. 2). Initiation of the secondary dispersion fan took place between three and one million years ago (Snelling, 1990). Presumably, transport started when the lower boundary of the weathering zone reached the top of the orebody and moving groundwater gained access to the uranium. The orebody in the unweathered zone seems to have remained intact for the past few million years (Payne and others, 1992; Sverjensky, 1992). This may be explained by the fact that the uranium minerals have only been in contact locally with flowing groundwater (in fractures). In other words, most of the uranium present in the unweathered zone was not available for transport. Therefore, the main hypothesis in this study is that transport of uranium occurs primarily in the weathering zone.

Leaching and transport of uranium and the formation of the dispersion fan is influenced by five major processes: groundwater flow, dissolution/precipitation, hydrodynamic dispersion, adsorption/desorption, and weathering. The role of groundwater flow is discussed briefly here. Other processes will be considered in the following sections.

In principle, in order to simulate the transport process, the present and past history of groundwater should be known. The present groundwater flow pattern has been studied through both field investigations and numerical modeling (Davis, Marley, and Norris, 1992; Townley and others, 1992). At present the general direction of groundwater flow in the weathering zone is believed to be from northeast to southwest, roughly parallel to the Koongarra Reverse Fault. Seasonal fluctuations in precipitation strongly influence surface runoff and groundwater flow in surficial sands. However, due to the existence of a confining layer (the weathered zone) groundwater flow in the weathering zone is hardly affected (Payne and others, 1992; Townley and Barr, 1992). The flow regime has undergone continuous changes in magnitude and direction during the past few million years and is

believed to be still in a transient state. Therefore, in principle, it is necessary to have an idea of the evolution of the groundwater flow patterns in the past. This, however, has proven to be an almost impossible task. Changes in groundwater flow have occurred as a result of climatic changes, tectonic activities, weathering, and filling of the Koongarra Fault. How these events have affected groundwater flow is not known. Because of these uncertainties, no attempt is made here to perform extensive groundwater flow modeling. However, advection is included in the transport modeling. Different values for the magnitude of groundwater velocity are used in the simulations.

ANALYSIS OF URANIUM DISTRIBUTION

A large number of chemical analyses of groundwater and the solid phase have been carried out (Murakami and others, 1992; Edis and others, 1992; Payne and others, 1992). A large data set is available on the concentration of uranium in the orebody and in the dispersion fan (Duerden, 1992). Because of the original interest in the exploration of uranium, the majority of concentration data relate to the solid phase and only a few measurements of the uranium concentration for the liquid phase have been made in the region of interest (Payne and others, 1992). In this section, a description of the form and distribution of uranium is given and results of an analysis of the measured uranium distribution are presented. Details of the analysis are given in van de Weerd and others (1994). The main purpose of the analysis has been to shed light on the history of the flow and transport and to estimate some chemical and physical parameters.

The form and abundance of mineral constituents greatly affect weathering processes, final products of weathering, groundwater chemistry, and uranium–mineral interaction (Edis and others, 1992). The quartz-chlorite schist, the host rock in Koongarra, varies in composition with depth as a result of weathering. Quartz has been resistant to weathering and persists even at the surface, while chlorite has been changed into clay and iron minerals (Airey, 1986). Above the No. 1 orebody, uranium is associated principally with phosphor and the uranyl phosphate mineral saleeite has been detected (Edis and others, 1992). Outside the region of the orebody, uranium is found to be associated mainly with iron oxides, but also with phosphate and magnesium minerals. Part of the uranium is nonaccessible to the liquid phase.

As transport is assumed to have stopped in the weathered zone, the distribution of uranium in this zone can be regarded as a record of concentrations in the weathering zone in the past. Of course, aging and ongoing weathering can cause a shift in the partitioning of uranium between the solid and liquid phase. However, the solid-phase uranium concentrations in the weathered zone are so large that they will hardly be influenced by this shift. Therefore, present day solid-phase uranium concentrations are viewed in this analysis as a record of past concentrations.

Figures 3A–3F show contours of measured solid-phase uranium concentrations at different depth intervals, ranging from the present ground surface to a depth of 30 m (just below the weathering zone). Each figure is based on measurements of average concentrations in cores of 5 m long. The positions of the observation points are indicated in the figures. Contours are based on interpolated values using inverse-distance-squared weights. In Figures 3B–3F the position of the orebody as specified in the numerical simulations is indicated as well. The outline of the orebody is based on a projection of the primary ore from the base of weathering to the surface (Pedersen, 1987). The orebody is not present in the first 5-m layer.

Figure 3F shows the distribution of solid-phase uranium in the unweathered zone. From this figure it appears that the occurrence of uranium is restricted to the close proximity of the orebody, consistent with the assumption that very little uranium transport has taken place in the unweathered zone (Payne and others, 1992). Figure 3E shows the solid-phase uranium concentrations in the weathering zone and Figures 3A–3D show the solid-phase uranium concentrations in the fully weathered layers above the weathering zone.

From Figures 3B–3D, it appears that the direction and extent of the dispersion fan in the fully weathered zone does not vary significantly with depth. It is possible that variability in uranium concentration with depth has been obscured because of the use of average values for 5-m intervals. Nevertheless, this observation provides clues to the history of flow and transport in the fully weathered zone. Assuming that the magnitude and direction of groundwater velocity has been constantly varying as the weathering process has moved downward, one would expect significant variations in the extent, form, and pattern of uranium distribution in the weathered layers. Thus, either average magnitude and direction of groundwater flow have changed little in the past two million years, or the characteristic time over which changes in groundwater flow pattern have occurred is small compared to the time required for a detectable transport of uranium in the weathering zone. That the extent and form of the dispersion fan in the fully weathered zone are independent of depth also supports the hypothesis that groundwater movement and transport of uranium has almost stopped in this zone. Significant transport in the fully weathered zone would have resulted in much larger transport distances in this zone, and a decreasing extent of the dispersion fan with depth; neither of these seem to be the case.

The form of the dispersion fan as shown in Figures 3A–3F allows us to estimate the main transport direction and average distance of transport. Measured from the center of the orebody and based on the shape and position of the 100 mg/kg solid-phase uranium contour, the principal transport direction, which is the direction of largest transport distance, is southwesterly: an average compass bearing of 215° with a maximum deviation of 6° . The average transport distance in that direction is about 340 m with a maximum deviation of 5 m. The extent of the dispersion fan and the average transport distance is controlled not only by the flow velocity, but also by chemical properties of the system.

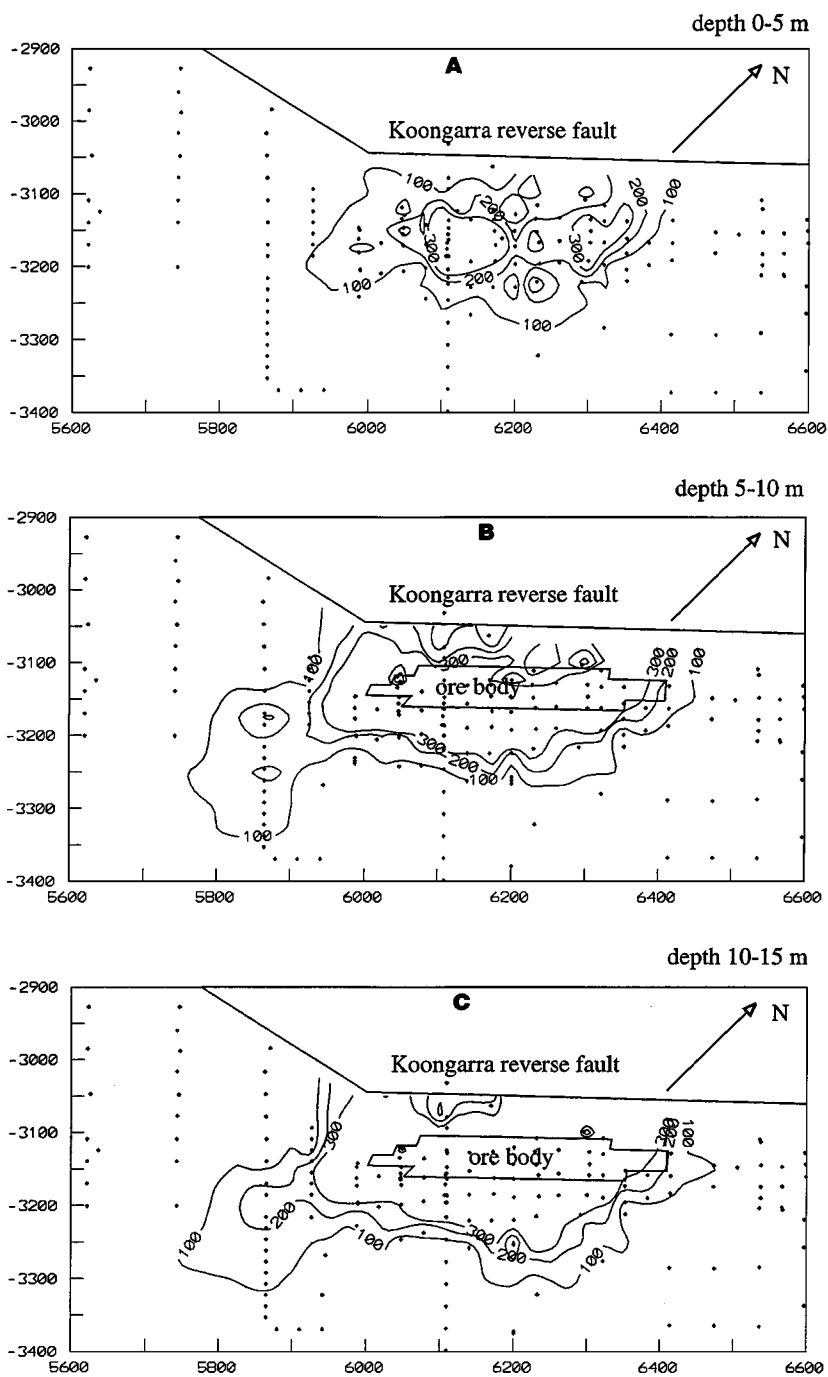


Figure 3. Contours of measured (A–F) and calculated (G–K) solid-phase uranium concentrations (mg/kg) averaged over 5 m intervals at different depths. Calculated values from run 9 (Table 1).

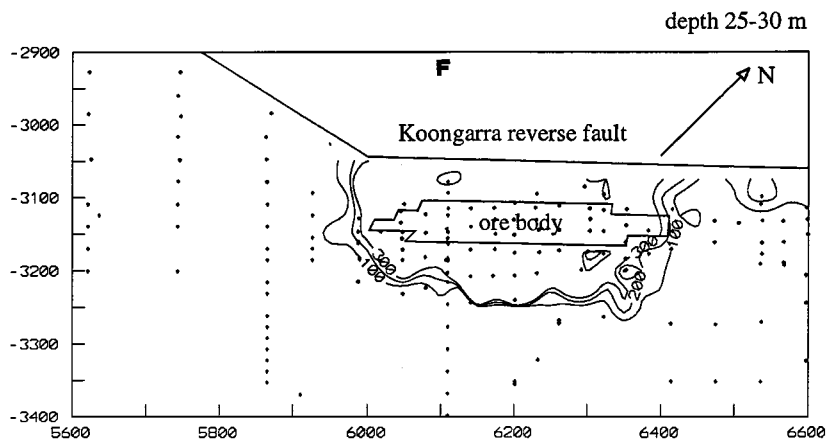
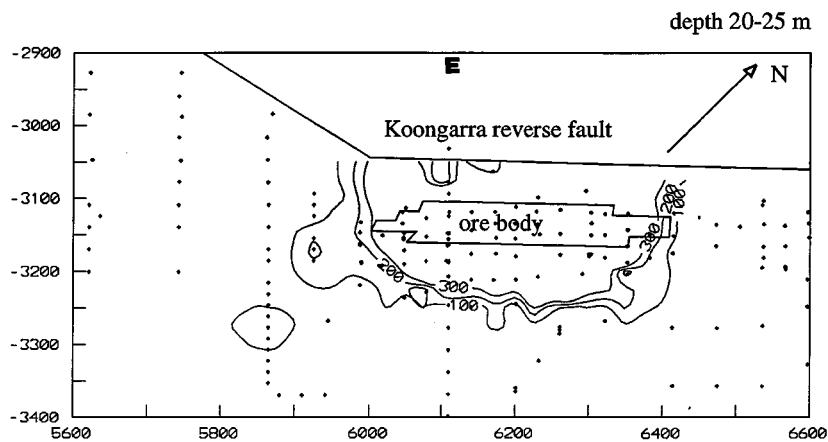
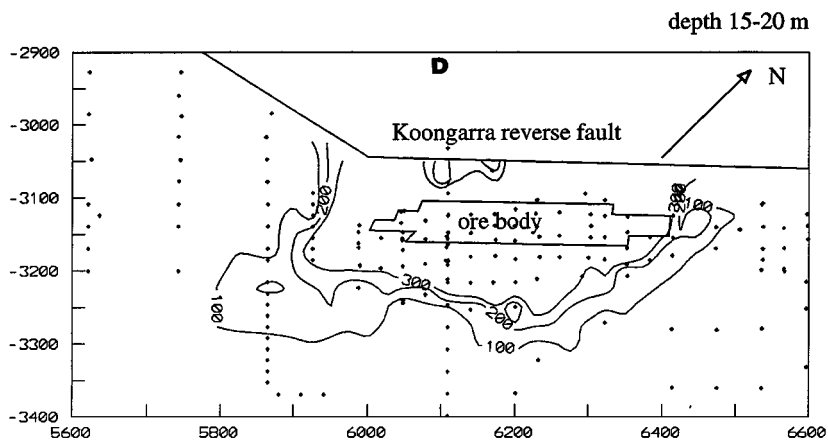


Figure 3. (Continued).

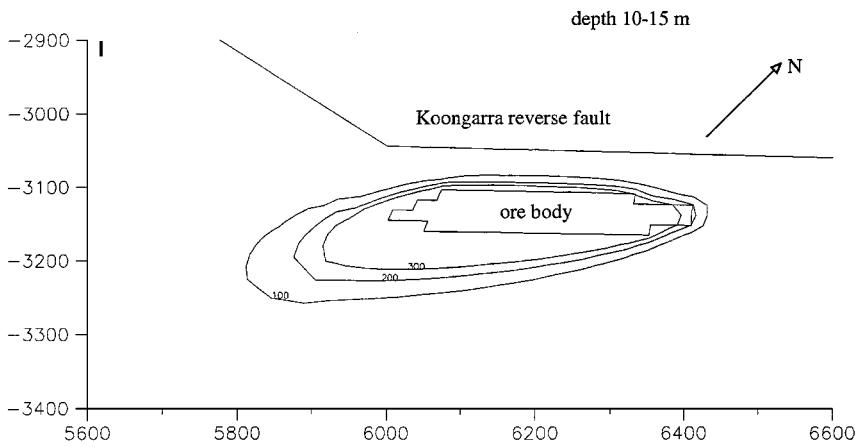
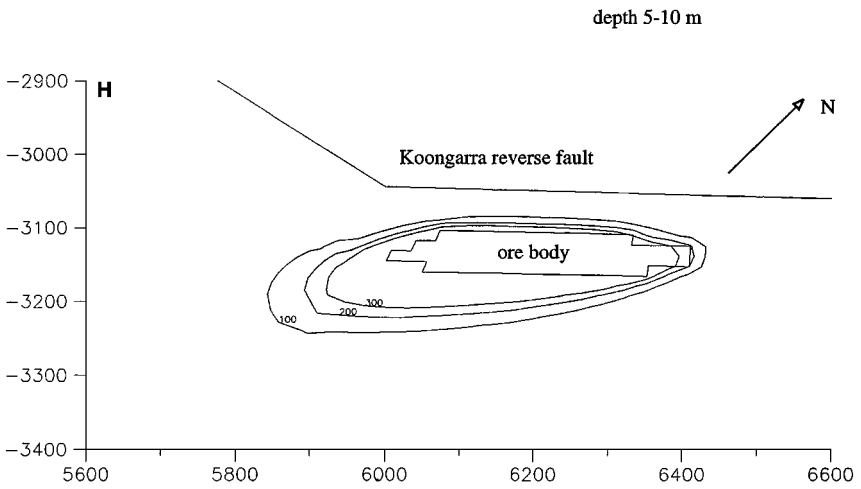
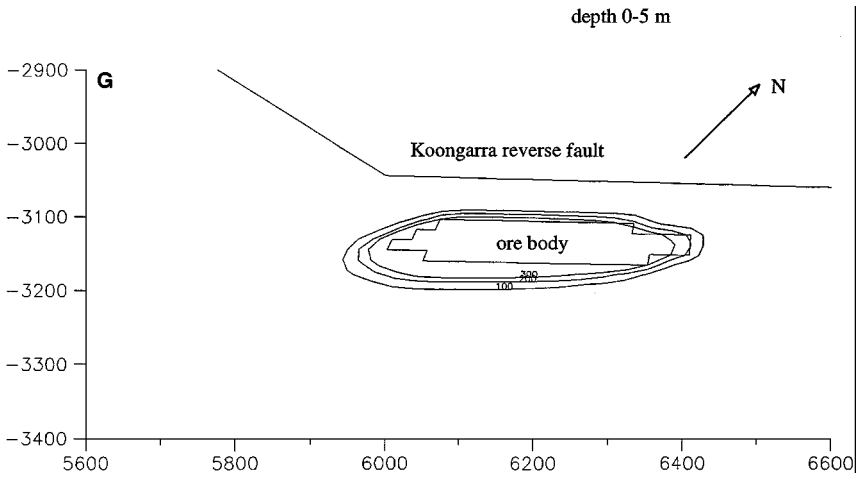


Figure 3. (Continued).

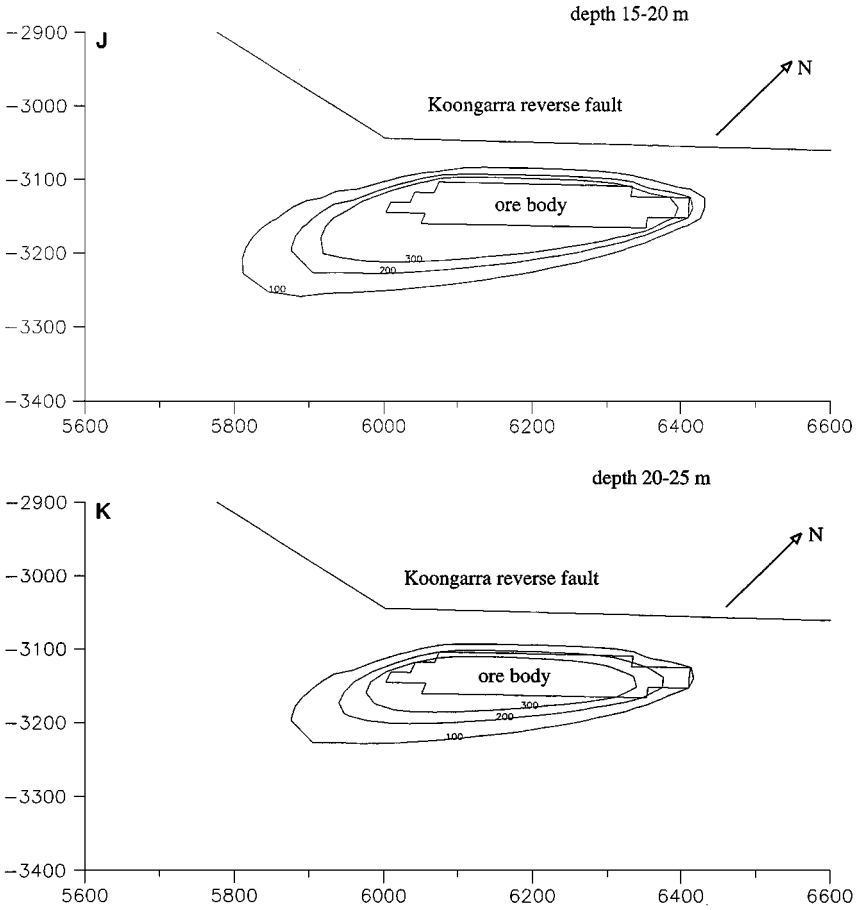


Figure 3. (Continued).

Koongarra groundwater is at present significantly undersaturated with respect to the major uranium minerals. Under such conditions, adsorption is likely to be a more important retardation mechanism than precipitation of uranium minerals (Payne and others, 1992). The initial retardation mechanism of uranium is suggested to be sorption to iron minerals precipitated during chlorite weathering. As weathering proceeds, aging of the iron oxides may occur, causing immobilization of uranium, i.e., incorporation of the uranium, which was initially sorbed, into the minerals (Edis and others, 1992). Although in the weathering zone immobilization might play a role, it has been neglected in this study. In the weathered zone uranium

distribution is not influenced by immobilization because almost no transport takes place in this zone.

An analysis of the partition coefficient, i.e., the ratio of solid- and liquid-phase uranium concentrations, may give an idea of the retardation of uranium in the system. A large variation in the value of the partition coefficient is found, depending on whether it is calculated on the basis of the total solid-phase uranium concentration or the accessible solid-phase uranium concentration (Edis and others, 1992). However, the partition coefficient measured outside the orebody seems to be independent of the uranium concentration, and shows no significant spatial trend (van de Weerd and others, 1994).

Because adsorption is likely to be a more important retardation mechanism for uranium than the precipitation of uranium minerals (Payne and others, 1992), and because no significant trend is found in the partition coefficient, it is assumed that retardation of uranium outside the orebody can be described by a linear relationship between solid- and liquid-phase concentrations. This is a relationship similar to the one often used to describe linear equilibrium sorption. The partition coefficient, commonly called the equilibrium distribution coefficient, is then denoted by K_d , which will also be used in this study. The nature of exchange between solid and liquid is, however, open to debate and may include other mechanisms beside sorption, even though sorption is probably the dominant process.

For the region inside the orebody we assume that interaction between solid-phase uranium and dissolved uranium is through dissolution only. Analysis of available data with the help of equilibrium geochemical calculations has shown that aqueous-phase uranium concentration in the region of the orebody is much lower than equilibrium concentration (van de Weerd and others, 1994). A possible and acceptable explanation for this difference is that the overall kinetics of dissolution of uranium minerals is relatively slow compared to the transport of uranium by flowing groundwater. Therefore, dissolution kinetics must be taken into account when modelling the transport of dissolved uranium.

A MATHEMATICAL MODEL OF URANIUM TRANSPORT IN KOONGARRA

We realize that the geohydrochemical processes that have occurred in Koongarra over the last two million years are extremely complicated. For instance, groundwater velocities, reaction rates, adsorption rates, and all other weathering processes have been variable in time and space. It is by no means possible to perform a quantitative modeling of the history of flow and transport of uranium in Koongarra. The philosophy of this study is to show that with a simple modeling concept and with many simplifying assumptions it is still possible to identify the most relevant processes and to capture the major trends in the spreading of uranium.

Derivation of the Transport Equation for the Weathering Zone

To describe the transport of uranium in the moving weathering zone, the following processes are considered: advective transport, diffusive and dispersive transport, interaction between liquid and solid phase, decay, and dissolution. In addition, we account for downward movement of the weathering zone. Assumptions employed in the development of the governing mass balance equation are as follows:

- interaction with the solid phase outside the orebody is given by a linear adsorption isotherm;
- overall dissolution of uranium in the orebody is described by a first-order kinetic relation;
- decay of uranium is given by a first-order relation;
- uranium is not produced by the decay of other species;
- the porous medium is saturated and the liquid density is constant in time and space.

For a linear adsorption isotherm, the retardation factor R is given by

$$R = 1 + \frac{\rho_s(1 - n)}{n} K_d \quad (1)$$

where ρ_s is the mass density of the solid, n is the porosity, and K_d is the equilibrium distribution coefficient. Both K_d and hence R are considered to be independent of the liquid-phase uranium concentration C .

For the purpose of this study we assume a linear kinetic relationship for the dissolution of uranium in the orebody:

$$S = nK(C_{\text{eq}} - C) \quad (2)$$

where S is the dissolution rate, K is the dissolution rate coefficient, C_{eq} is the equilibrium concentration of uranium under given conditions, and C is the uranium concentration in the liquid phase. Note that Equation (2) assumes that there is always a sufficient amount of mineral available to sustain a positive value of S . Otherwise, the source term should go to zero when the mineral is depleted. In that case a mass balance equation for the solid-phase mineral must be included.

Under these assumptions, the three-dimensional mass balance equation for dissolved uranium can be written as

$$\frac{\partial}{\partial t}(nRC) + \nabla \cdot (\mathbf{q}C) + \nabla \cdot \mathbf{J} + nR\lambda C - nK(C_{\text{eq}} - C) = 0 \quad (3)$$

where \mathbf{q} is the Darcy velocity, which is assumed to be a (known) function of space and time, \mathbf{J} is the dispersive mass flux, and λ is the decay coefficient of uranium. Commonly, the dispersive mass flux \mathbf{J} is described by a Fickian-type relation.

Simulation of (3) over the full three-dimensional domain would constitute excessive computational effort and is not necessary for practical purposes. Because of the confining effect of the fully weathered and the unweathered zones, it is believed that the flow is mainly horizontal in the transitional weathering zone and that transport of uranium in the vertical direction is negligible. Under these conditions it is sufficient to simulate the uranium transport in the weathering zone only, and then as a two-dimensional process. For this purpose, it is necessary to derive a two-dimensional version of Equation (3), which takes into account the downward movement of the weathering zone. This can be achieved by averaging Equation (3) in the vertical direction.

Taking the positive z -direction downward, integration of (3) over the thickness of the moving weathering zone yields:

$$\int_{z_t}^{z_b} \frac{\partial}{\partial t} (nRC) dz + \int_{z_t}^{z_b} \nabla \cdot (\mathbf{q}C) dz + \int_{z_t}^{z_b} \nabla \cdot \mathbf{J} dz + \int_{z_t}^{z_b} nR\lambda C dz - \int_{z_t}^{z_b} nK(C_{eq} - C) dz = 0 \quad (4)$$

where z_t and z_b are the z -coordinates of top and bottom boundaries of the weathering zone, respectively. Both are considered to be functions of space and time.

The integrals of derivatives in Equation (4) can be written in terms of derivatives of integrals by making use of the integral theorems as developed by Gray and others (1993). The resulting equation can be written as

$$\begin{aligned} \frac{\partial}{\partial t} \left[\int_{z_t}^{z_b} nRC dz \right] + \nabla_{xy} \cdot \left[\int_{z_t}^{z_b} \mathbf{q}C dz \right] + \nabla_{xy} \cdot \left[\int_{z_t}^{z_b} \mathbf{J} dz \right] \\ + \int_{z_t}^{z_b} nR\lambda C dz - \int_{z_t}^{z_b} nK(C_{eq} - C) dz \\ + \left[\frac{\mathbf{N} \cdot \mathbf{q}}{\mathbf{e}_z \cdot \mathbf{N}} C + \frac{\mathbf{N} \cdot \mathbf{J}}{\mathbf{e}_z \cdot \mathbf{N}} - \frac{\mathbf{N} \cdot \mathbf{w}}{\mathbf{e}_z \cdot \mathbf{N}} nRC \right]_{bot} \\ - \left[\frac{\mathbf{N} \cdot \mathbf{q}}{\mathbf{e}_z \cdot \mathbf{N}} C + \frac{\mathbf{N} \cdot \mathbf{J}}{\mathbf{e}_z \cdot \mathbf{N}} - \frac{\mathbf{N} \cdot \mathbf{w}}{\mathbf{e}_z \cdot \mathbf{N}} nRC \right]_{top} = 0 \quad (5) \end{aligned}$$

where \mathbf{N} is a unit vector normal to the (top or bottom) boundary of the weathering zone, pointing outward, \mathbf{e}_z is a unit vector in the positive z direction, \mathbf{w} is the vertical velocity of the weathering zone, ∇_{xy} is the divergence operator in the xy

(horizontal) direction, and the subscripts “*bot*” and “*top*” indicate that the term in brackets needs to be evaluated at the bottom and the top of the weathering zone, respectively.

Average values over the thickness of the weathering zone are now defined such that the resulting two-dimensional (2D) equations are similar in form to the three-dimensional mass balance equation. With thickness of the weathering zone denoted by $b = z_b - z_t$, the following average values are defined:

$$\langle n \rangle = \frac{1}{b} \int_{z_t}^{z_b} n dz \quad (6a)$$

$$\langle C \rangle = \frac{1}{b \langle n \rangle} \int_{z_t}^{z_b} n C dz \quad (6b)$$

$$\langle R \rangle = \frac{1}{b \langle n \rangle \langle C \rangle} \int_{z_t}^{z_b} n R C dz \quad (6c)$$

$$\langle \mathbf{q} \rangle = \frac{1}{b} \int_{z_t}^{z_b} \mathbf{q} dz \quad (6d)$$

$$\langle \mathbf{J} \rangle = \frac{1}{b} \left[\int_{z_t}^{z_b} \mathbf{J} dz + \int_{z_t}^{z_b} (\mathbf{q} - \langle \mathbf{q} \rangle) (C - \langle C \rangle) dz \right] \quad (6e)$$

$$\langle K \rangle = \frac{1}{b \langle n \rangle (\langle C_{eq} \rangle - \langle C \rangle)} \int_{z_t}^{z_b} n K (C_{eq} - C) dz \quad (6f)$$

where $\langle \cdot \rangle$ indicates an average value over the thickness of the weathering zone. In defining the average values the following criteria have been employed:

- The average value of the retardation factor (R) is defined to be the ratio of the total mass of the solute in the system to the mass of solute in the liquid phase.
- The average value of the dispersive mass flux (\mathbf{J}) includes a term that accounts for a possible correlation between variations in the specific discharge and variations in the concentration in the liquid phase.
- The average value of the dissolution constant (K) relates the total source term to the difference between the average equilibrium concentration (C_{eq})

and the average value of the concentration $\langle C \rangle$. Note that $\langle C_{eq} \rangle$ is defined similarly to $\langle C \rangle$.

To simplify the analysis, the following assumptions are made:

- Both the top boundary and the bottom boundary of the weathering zone are horizontal.
- Top and bottom boundaries of the weathering zone move with the same velocity, which is given by $\mathbf{w} = (0, 0, w)$ such that a positive value of w indicates downward movement.
- Vertical velocity of the liquid phase at the top and bottom boundaries of the weathering zone equals the downward velocity of these boundaries, i.e., $q_z = nw$, where q_z is positive downward.

From these assumptions, it follows that at the bottom of the weathering zone $\mathbf{e}_z \cdot \mathbf{N} = 1$, $\mathbf{N} \cdot \mathbf{w} = w$, $\mathbf{N} \cdot \mathbf{q} = q_z$ and $\mathbf{N} \cdot \mathbf{J} = J_z$, and at the top of the weathering zone $\mathbf{e}_z \cdot \mathbf{N} = -1$, $\mathbf{N} \cdot \mathbf{w} = -w$, $\mathbf{N} \cdot \mathbf{q} = -q_z$ and $\mathbf{N} \cdot \mathbf{J} = -J_z$. Furthermore, the thickness b of the weathering zone is constant.

With these assumptions, the resulting 2D mass balance equation is given by

$$\begin{aligned} \frac{\partial}{\partial t} (\langle n \rangle \langle R \rangle \langle C \rangle) + \nabla \cdot (\langle \mathbf{q} \rangle \langle C \rangle) + \nabla \cdot \langle \mathbf{J} \rangle \\ + \langle n \rangle \langle R \rangle \lambda \langle C \rangle - \langle n \rangle \langle K \rangle (\langle C_{eq} \rangle - \langle C \rangle) \\ + \frac{1}{b} [nw(R-1)C - J_z]_{top} - \frac{1}{b} [nw(R-1)C - J_z]_{bot} = 0 \end{aligned} \quad (7)$$

To estimate the advective terms $nw(R-1)C$ at the top and bottom of the weathering zone, we assume that the concentration is locally a linear function of the z -coordinate, such that concentration at the top of the weathering zone can be written as

$$C_{top} = 2\langle C \rangle - C_{bot} \quad (8)$$

Furthermore, it is assumed that the local value of the retardation factor R equals the average value of R , and that uranium concentration in the unweathered zone below the weathering zone, i.e., C_{bot} , is zero outside the region of the orebody. With these assumptions, the advective term at the top boundary equals $2nw(R-1)\langle C \rangle$. Inside the region of the orebody, all uranium associated with the solid phase is assumed to be present as minerals. Interaction with the liquid phase is then through the dissolution term only hence $R = 1$ inside the orebody. Consequently, the advective term evaluated at the bottom of the weathering zone is zero everywhere.

If the vertical mass flux J_z is due to diffusion only, J_z is some three orders of magnitude smaller than the advective term $nw(R-1)\langle C \rangle$ at the top of the

weathering zone for the values of the physical/chemical parameters used in this study. Consequently, these diffusive mass fluxes may be neglected. The final form of the 2D mass balance equation is then given by

$$\frac{\partial}{\partial t}(nRC) + \nabla \cdot (\mathbf{q}C) + \nabla \cdot \mathbf{J} + nR\lambda C - nK(C_{\text{eq}} - C) + \frac{2nw(R-1)}{b}C = 0 \quad (9)$$

where the averaging symbols have been omitted for clarity of notation.

The fifth term on the left-hand side of Equation (9) is a source term accounting for dissolution of uranium in the orebody. The last term on the left-hand side of Equation (9) is a sink term accounting for sorbed uranium leaving the model domain at the top of the moving weathering zone.

Finally, we assume that the dispersive mass flux in Equation (9) is described by a Fickian-type relation. The dispersion tensor \mathbf{D} is defined as a function of the Darcy velocity by the well-known relationship (Bear, 1979)

$$\mathbf{D} = (nD_m + \alpha_T|\mathbf{q}|)\mathbf{I} + (\alpha_L - \alpha_T)\frac{\mathbf{q}\mathbf{q}}{|\mathbf{q}|} \quad (10)$$

where D_m is the effective diffusion coefficient, \mathbf{I} is the unit tensor, α_L is longitudinal dispersivity, and α_T transversal dispersivity. Note that the effect of tortuosity of the porous medium is included in the effective diffusion coefficient D_m . To solve Equation (9) appropriate initial and boundary conditions must be determined.

Numerical Simulations

The main purpose of this work has been to assess the ability of a rather simple transport model to account for the observed distribution of uranium in the Koongarra system. We are aware of the fact that the processes occurring in the Koongarra system are very complex. Because of large temporal and spatial variations in physical-chemical conditions (e.g., pH, Eh, pCO₂, uranium mineralogy, and mineral composition of the host rock), large temporal and spatial variations in model parameters such as K_d , C_{eq} , K , v , n , and w may have occurred. Although it is impossible to reconstruct the details of past history of flow and transport, it should be possible to identify the dominant processes and simulate the main features of the dispersion fan with a simplified model using constant values for model parameters.

The 2D model domain is bounded by the Koongarra fault, the Koongarra Creek, and the two ephemeral creeks perpendicular to the Koongarra fault (Fig. 4). These boundaries coincide with assumed hydrological boundaries. The finite

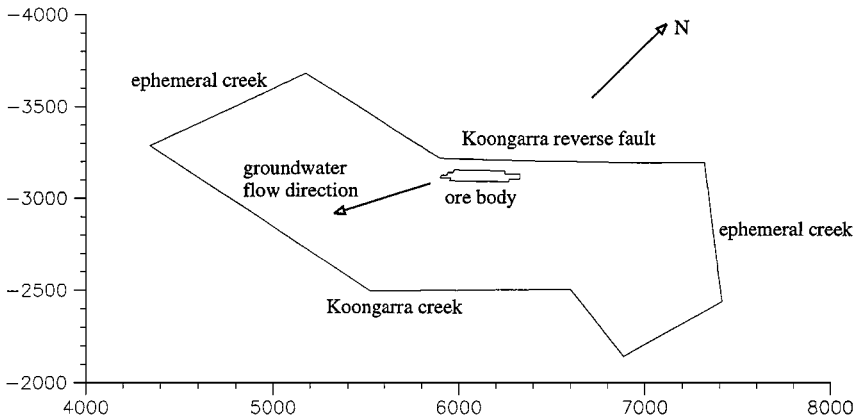


Figure 4. Model domain and average groundwater flow direction.

element mesh used for simulations consists of 1376 quadrilateral elements and 1452 nodes and is refined in the region of the orebody. Boundaries of the orebody are based on a projection of the primary ore from the base of weathering to the surface (Pedersen, 1987). Therefore, these areal boundaries are constant with depth.

The starting time for transient simulations is taken to be the time that the weathering zone reached the top of the orebody, 1.8 million years ago (van de Weerd and others, 1994). It is assumed that at that time, the top boundary of the weathering zone corresponded with the present ground surface. Because of the assumed constant rate of downward movement of the weathering zone, any given time in the simulations corresponds to a certain depth; the relationship is through the weathering velocity w . Thus, with the assumption that no transport of uranium takes place in the fully weathered zone, calculated uranium distribution at a certain time can be compared with present day measured uranium concentrations at the corresponding depth. The transformation from calculated uranium concentrations in the weathering zone at a certain time to present uranium concentrations in the fully weathered zone at a certain depth proceeds as follows. At time t after start of the simulation, the top of the weathering zone is at a depth of wt below ground surface. At that time, the uranium concentration at the top of the weathering zone is according to Equation (8) two times the average uranium concentration in the weathering zone (since $C_{bot} = 0$). This is assumed to give the concentration in the fully weathered zone, because the concentration is not expected to change once the weathering front has passed this depth. The linear relation (8) is used to determine the uranium concentration for the present position of the weathering zone.

Boundary conditions for all simulations are taken to be a no-dispersive mass flux across all boundaries. For the initial conditions, uranium concentrations in the liquid phase have been set to zero everywhere.

The approach taken in this study is to estimate values of the physical and chemical parameters for the weathering zone on the basis of available data, and to investigate sensitivity of the model results to these values. Parameters whose values have been varied in this study are equilibrium distribution coefficient K_d , groundwater velocity \mathbf{q} , movement of the weathering zone w , and dissolution rate constant of uranium in the orebody K . All properties are assumed to be constant in space and time.

The value of the effective molecular diffusion coefficient was chosen to be 10^{-9} m²/s; its effect will be small compared to the effect of dispersion. The values of the longitudinal dispersivity, α_L and the transversal dispersivity, α_T were arbitrarily set equal to 30 and 3 m, respectively.

The half-life of uranium is known to be $4.5 \cdot 10^9$ years. Consequently, the decay term λnRC will not play a role given the duration of the simulation period ($1.8 \cdot 10^6$ years). The decay of uranium accounts for removal of only 0.05% of the total uranium present in the system; nevertheless, this effect is included in the computations.

Thickness of the weathering zone b is assumed to be constant in time and space, and is estimated to be 5 m, based on present day observations (Emerson and others, 1992).

According to Edis and others (1992), the partition coefficient (based on accessible solid-phase uranium concentration) varies in the range of 0.4–1 m³/kg. Therefore, a reasonable estimate of the average equilibrium adsorption coefficient K_d is 0.7 m³/kg. Simulations have also been carried out with K_d values of 1.5 and 2 m³/kg respectively. With the density of the solid material $\rho_s = 2660$ kg/m³ and a porosity of $n = 0.15$ (Emerson and others, 1992), the retardation factor R varies from 10550 to 30150. In the region of the orebody, the retardation factor R is assumed to be equal to one (no adsorption).

Because available hydrological data are scarce and incomplete, especially with regard to the boundary conditions, it is difficult to determine even the present day velocity field. To determine variations in the velocity field over the past 2 million years, detailed information about past climate changes and their impact on the groundwater flow regime would be needed. In the absence of such information, the groundwater flow rate has been assumed to be constant in space and time. This is a very crude first approximation to the “real” velocity field. Townley and Barr (1992) estimated the present groundwater velocity to be 1.3 m/yr in the southeast direction, more or less parallel to the Koongarra fault. This value has been used in our base case simulation. In some other simulations, velocity values have been increased to 13 m/yr in an attempt to obtain a better fit with the measured uranium concentrations. This is an arbitrary choice, but we feel that such a change in the groundwater velocity is allowable in view of the large variations that have occurred in the past.

It is considered that the weathering zone reached the top of the orebody about 1.8 million years ago, and since then it has moved downward about 20 m

Table 1. Model Parameters Used for Model Calculations with a Moving Weathering Zone

| Simulation no. | K (yr ⁻¹) | K_d (m ³ /Kg) | v_w (m/yr) | w (m/yr) |
|----------------|-------------------------|----------------------------|--------------|---------------------|
| 1 | 0.003 | 0.7 | 1.3 | $1.1 \cdot 10^{-5}$ |
| 2 | 0.003 | 0.7 | 1.3 | $5.5 \cdot 10^{-6}$ |
| 3 | 0.003 | 0.7 | 1.3 | $1.7 \cdot 10^{-5}$ |
| 4 | 0.003 | 1.5 | 1.3 | $1.1 \cdot 10^{-5}$ |
| 5 | 0.003 | 2.0 | 1.3 | $1.1 \cdot 10^{-5}$ |
| 6 | 0.0003 | 0.7 | 1.3 | $1.1 \cdot 10^{-5}$ |
| 7 | 0.03 | 0.7 | 1.3 | $1.1 \cdot 10^{-5}$ |
| 8 | 0.02 | 2.0 | 13 | $1.1 \cdot 10^{-5}$ |
| 9 | 0.025 | 2.0 | 13 | $1.1 \cdot 10^{-5}$ |
| 10 | 0.03 | 2.0 | 13 | $1.1 \cdot 10^{-5}$ |

to the current depth of the weathering zone. This leads to an average downward velocity of the weathering zone of $1.1 \cdot 10^{-5}$ m/yr. To investigate the effect of this downward velocity, simulations also have been carried out with downward velocities of $5.5 \cdot 10^{-6}$ and $1.7 \cdot 10^{-5}$ m/yr.

Dissolution of uranium in the orebody is controlled by the dissolution rate coefficient K and equilibrium concentration C_{eq} . Equilibrium geochemical calculations for the primary uranium mineral uraninite and solution properties (pH, Eh, HCO_3^- concentration) observed in boreholes situated in the orebody, have shown that a reasonable estimate of C_{eq} is 1300 mg/m³ (van de Weerd and others, 1994). The dissolution rate coefficient is more difficult to estimate. Various arbitrary values for K ranging from 0.0003 to 0.03 yr⁻¹ have been used in the simulations.

A total of 10 simulations were carried out with the parameter values given in Table 1. Simulation 1 serves as the base case. Simulations 1–3 consider the effect of the downward velocity of the moving weathering zone. Simulations 1, 4 and 5 relate to the effect of the equilibrium distribution coefficient K_d , while simulations 1, 6, and 7 consider changes in the value of the dissolution rate constant K . Based on results obtained from these computations, simulations 8–10 were performed with different values for the dissolution rate constant K and an increased equilibrium distribution coefficient and groundwater flow rate v_w . Note that the groundwater flow rate v_w given in Table 1 is related to Darcy flux used in Equation (9) by $q = nv_w$ where n is porosity, constant in space and time.

SIMULATION RESULTS AND DISCUSSION

In simulations carried out in this study, liquid-phase uranium concentrations are calculated. However, because the liquid-phase concentration measurements

are only a few and are not very reliable, comparison of calculated liquid-phase concentration with data is not helpful. Instead, for the purpose of comparison with data, simulation results will be converted to and presented in terms of solid-phase uranium concentrations using the K_d value of the corresponding simulation. These are then compared to solid-phase measurements which are more abundant and more reliable. In the region of the orebody, solid-phase concentration cannot be calculated because a mass balance equation for the solid minerals is not included in our model. In this region, liquid-phase data and calculation results will be compared.

The results of the simulations will be presented in two different ways. First, variation in uranium concentration with depth will be given for three different points in the domain: one point in the orebody, and two points at a distances of 60 and 200 m from the boundary of the orebody in the downstream direction. Second, contours of uranium concentration in the solid phase calculated in our “best fit” simulation are given at various depths.

Three simulations were carried out to investigate the effect of the downward velocity of the weathering zone, i.e., the weathering rate (simulations 1–3). In these simulations, the dissolution rate coefficient K is chosen sufficiently low such that the aqueous uranium concentration in the orebody will not reach the equilibrium concentration C_{eq} . Increasing the downward velocity of the zone results in an increase of the sink term in Equation (9). Consequently, resulting concentrations in the liquid phase are smaller at higher velocities of the weathering zone. Figure 5 shows uranium concentration as a function of depth in the three points mentioned above. Note the different scales for uranium concentrations in the figures. Also note that a pseudo-steady state situation is reached faster for larger velocities of the weathering zone. Because total simulation time is the same for all simulations, different values of the velocity of the weathering zone results in different depths of the weathering zone at the end of the simulation. Also note that no pseudo-steady state situation would have been reached if movement of the weathering zone had not been included in the model (i.e., $w = 0$).

The effect of adsorption has been investigated by increasing the equilibrium distribution coefficient K_d (simulations 1, 4, and 5). Figure 6 shows the results of these simulations. An increase in the distribution coefficient results in an increase in the retardation factor and hence in a decrease of the transport distance. Consequently, an increased value of K_d decreases both aqueous- and solid-phase uranium concentration at a certain point away from the orebody.

The effect of the rate of dissolution of uranium in the orebody has been investigated by changing the dissolution rate coefficient K (simulations 1, 6, and 7). Figure 7 shows the effect for the three points in the domain. An increase in the dissolution rate coefficient increases the source term in Equation (9). Consequently, concentrations in the system increase with K .

The extent of the dispersion fan in the first seven simulations was not large enough compared with the observations. To increase travel distance, average flow

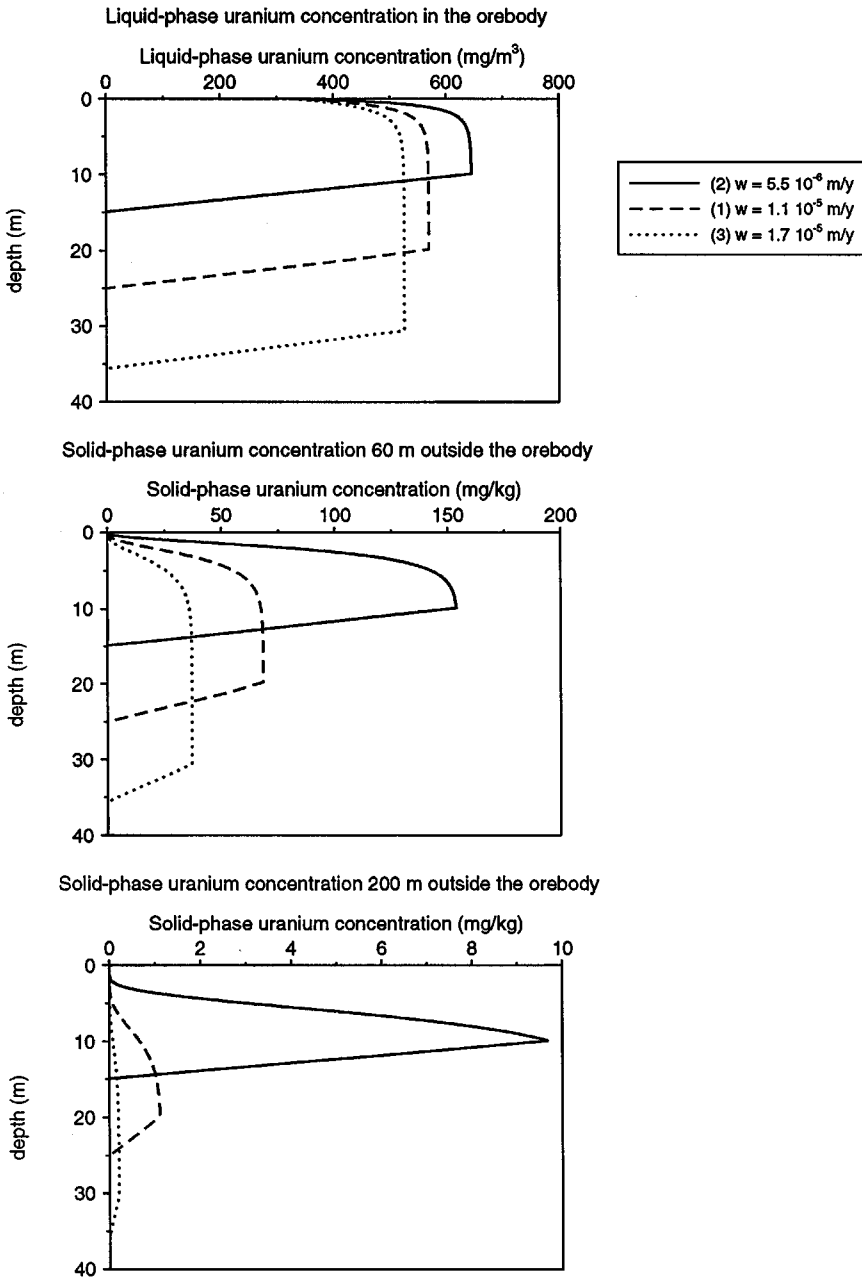


Figure 5. Effect of the downward velocity of the weathering zone on uranium concentrations; runs 1-3 (Table 1).

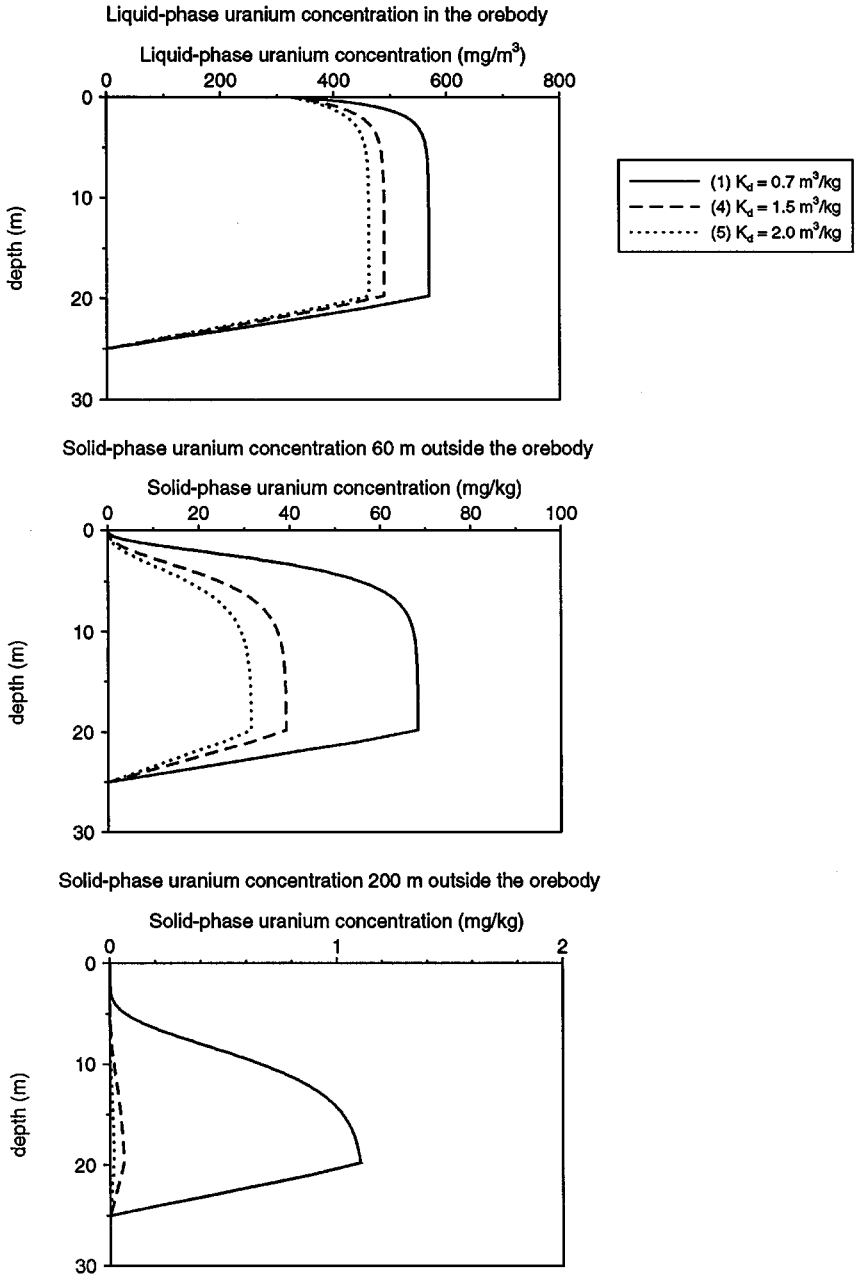


Figure 6. Effect of equilibrium distribution coefficient on uranium concentrations; runs 1, 4, and 5 (Table 1).

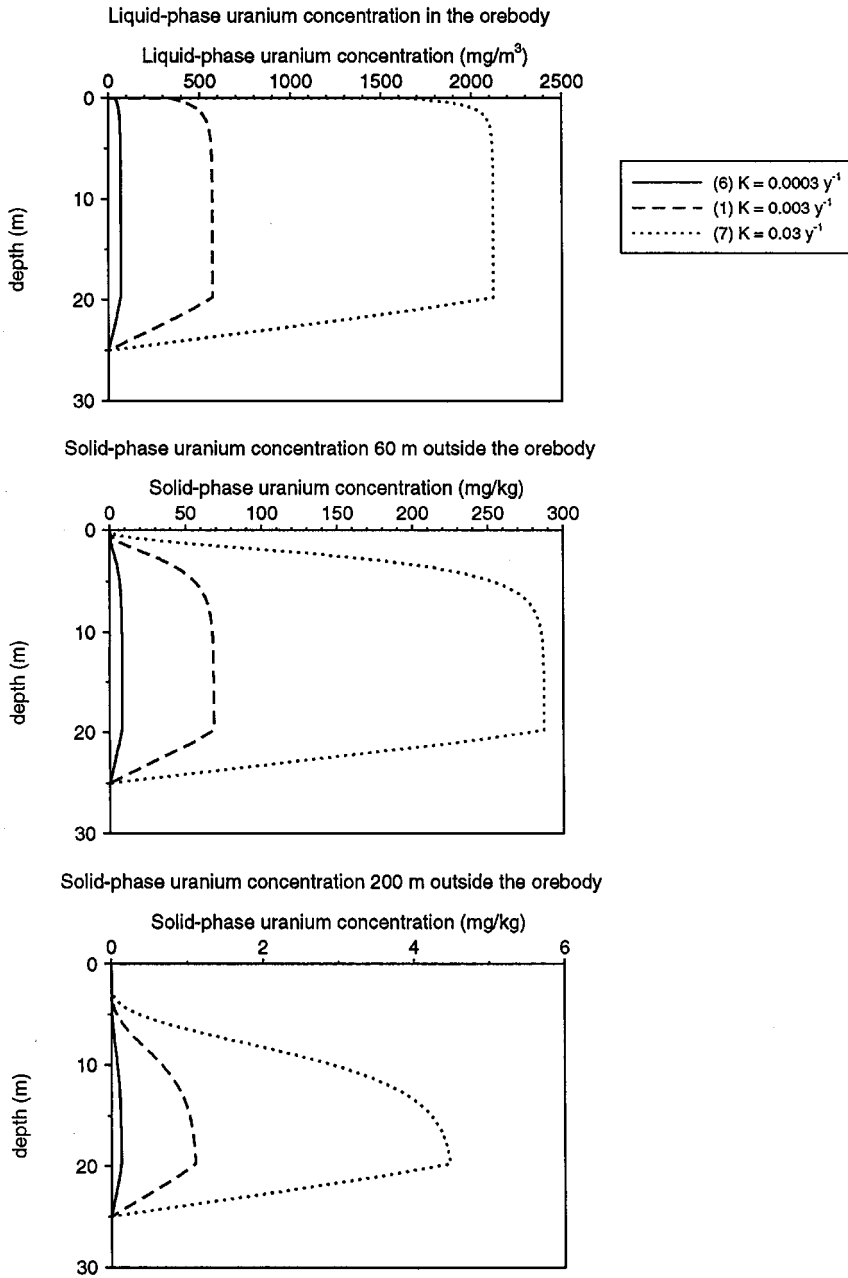


Figure 7. Effect of the dissolution rate coefficient on uranium concentrations; runs 1, 6, and 7 (Table 1).

velocity had to be increased. Therefore, in the next set of simulations (8–10), groundwater flow velocity was increased tenfold to 13 m/yr. This resulted, however, in too high values of the concentration in the dispersion fan. To compensate for this effect, the equilibrium distribution coefficient had to be increased threefold to $2 \text{ m}^3/\text{kg}$. One effect of increasing the groundwater velocity is that the transport of uranium away from the orebody is enhanced, thus decreasing the concentration in the orebody. To counteract this effect, the dissolution rate coefficient K was increased to 0.02, 0.025, and 0.03 y^{-1} , respectively. Figure 8 shows the results of these simulations. Observed values for the solid-phase uranium concentrations (Figures 8B and 8C) are based on interpolated measurements as shown in Figures 3A–3F. No consistent spatial distribution of the measured liquid-phase uranium concentration in the orebody can be obtained because of the limited number of measurements in the region of interest, and the large variation in these measurements. Therefore, in Figure 8A all available measurements in wells in this region are shown (Payne and others, 1992). Variations in these measurement are also shown. Computed values of the liquid-phase uranium concentrations in simulation 9 are in agreement with the maximum value measured in the orebody. From Figures 8B and 8C it appears that on the whole, simulation 9 shows a reasonable agreement with the measurements.

Results of simulation 9 as contours of the solid-phase uranium concentration at different depths are shown in Figures 3G–3K. These figures should be compared with the measured solid-phase concentrations shown in Figures 3A–3F. Here also it appears that the results of simulation 9 reasonably reproduces the spatial pattern of the uranium distribution at various depths.

Both the profiles of uranium concentration with depth and the contours of the solid-phase uranium concentration show that after about 500,000 years (equivalent to a depth of 5–10 m below ground surface) a pseudo-steady state distribution in the moving weathering zone is reached. This is because movement of the weathering zone introduces a sink term in the mass balance equation; when this balances uranium transport, a stationary situation occurs.

Given that a very simple model was used to simulate uranium transport in the past 1.8 million years, we have neither attempted to “fine tune” the parameter values nor relax the assumptions in order to obtain a better fit. For instance, adopting a different relationship for the uranium concentration as a function of depth in the weathering zone would influence both the sink term in the governing mass balance equation and the transformation from average uranium concentration in the weathering zone at a specific time to uranium concentration in the fully weathered zone at the corresponding depth.

Given the simplifying assumptions made, there is obviously no unique set of parameter values that will give a reasonable fit. The main features of the dispersion fan, however, have been simulated with a set of parameter values that are reasonable considering the available field data.

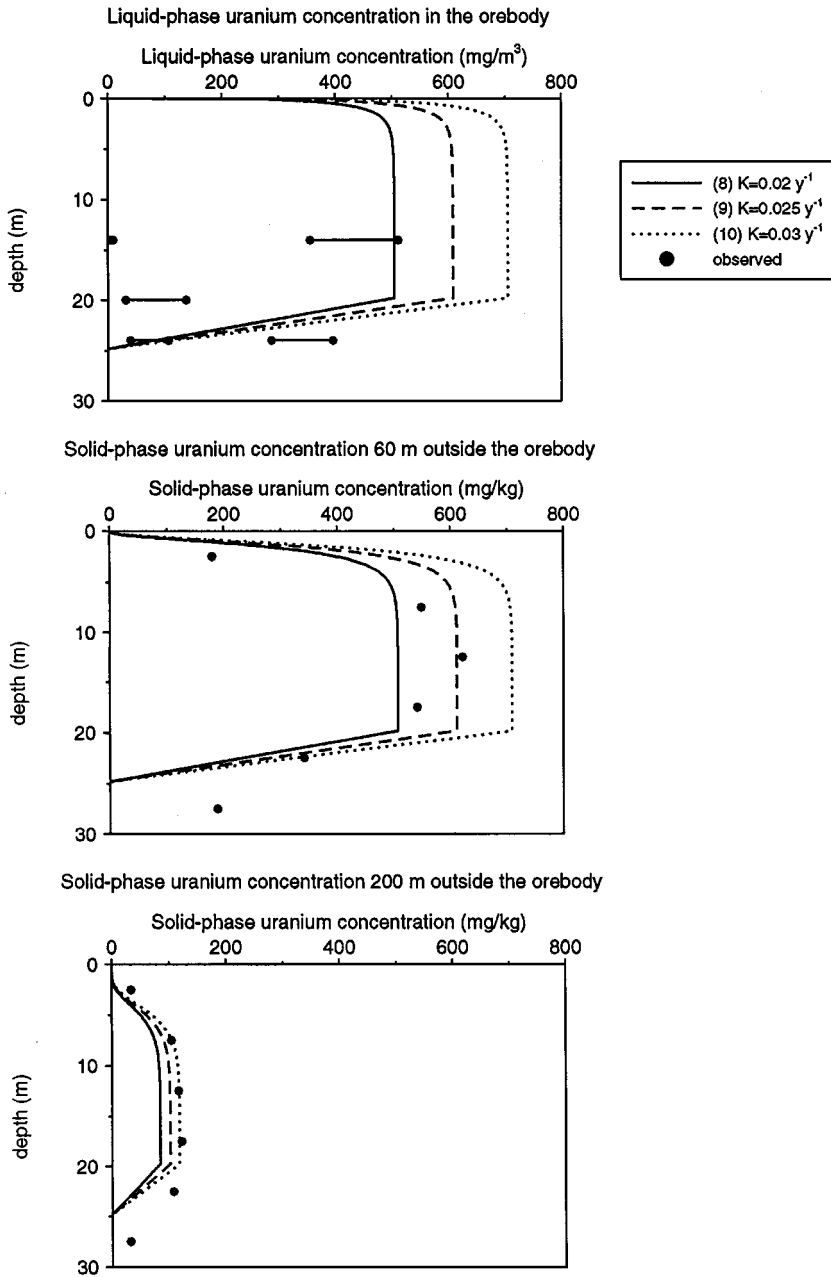


Figure 8. Results of simulations with different values of K and with $v_w=13 \text{ m}/\text{yr}$ and $K_d = 2 \text{ m}^3/\text{kg}$; runs 8, 9, and 10 (Table 1).

CONCLUSIONS

A reasonably simple model has been constructed to analyze the distribution of dispersed uranium at Koongarra. Even for the large simulation times, it appears that the use of an average constant groundwater velocity is adequate to obtain a uranium distribution very similar to the measured distribution. This probably means that the magnitude and direction of the groundwater flow averaged over characteristic time periods of $t_r = 4.5 \cdot 10^5$ years have not changed very much during the past two million years or that the times over which changes in the groundwater flow took place are small compared to the time required for a significant transport of uranium in the weathering zone.

Both the movement of the weathering zone and the kinetics of uranium dissolution in the orebody play an important role in the formation of the dispersion fan. The more or less uniform uranium distribution with depth can be explained by downward movement of the weathering zone.

ACKNOWLEDGMENTS

This work has been carried out in the framework of the RIVM participation in the INTRAVAL project. It has been commissioned by the Dutch Ministry of Housing, Physical Planning and Environment, and was partly funded by the Dutch Ministry of Economic Affairs as part of the radioactive waste research program OPLA. Mart Oostrom has assisted with some preliminary simulation attempts. His contribution is appreciated.

REFERENCES

- Airey, P. L., 1986, Radionuclide migration around uranium ore bodies in the Alligator Rivers Region of the Northern Territory of Australia—Analogue of radioactive waste repositories—A review: *Chem. Geology*, v. 55, p. 255–268.
- Bear, J., 1979, *Hydraulics of groundwater*: McGraw-Hill, New York, 234 p.
- Davis, S. N., Marley, R. D., and Norris, J. R., 1992, *Hydrogeological field studies: Alligator Rivers Analogue Project Final Report, Volume 5*, Australian Nuclear Science and Technology Organisation (ANSTO), 174 p.
- Duerden, P., 1992, *The Alligator Rivers Natural Analogue Project: The International INTRAVAL Project, Phase 1, Test case 8*, Organisation for Economic Co-operation and Development (OECD)/Nuclear Energy Agency (NEA), 215 p.
- Edis, R., Cao, L. Q., Cashion, J., Klessa, D., Koppi, A. J., Murakami, T., Nightingale, T., Payne, T., Snelling, A., and Yanase, N., 1992, *Chemistry and mineralogy of rocks and soil: Alligator Rivers Analogue Project Final Report, Volume 8*, Australian Nuclear Science and Technology Organisation (ANSTO), 255 p.
- Emerson, D. W., Mills, K. J., Miyakawa, K., Hallett, M. S., Cao, L. Q., 1992, *Geophysics, petrophysics and structure: Alligator Rivers Analogue Project Final Report, Volume 4*, Australian Nuclear Science and Technology Organisation (ANSTO), 125 p.

- Gray, W. G., Leijnse, A., Kolar, R. L., and Blain, C. A., 1993, Mathematical tools for changing spatial scales in the analysis of physical systems. CRC Press, Boca Raton, FL, 232 p.
- International Atomic Energy Agency, 1981, Safety assessment for the underground disposal of radioactive wastes: Int. Atomic Energy Agency, Rep. 56, Vienna, 32 p.
- Murakami, T., Isobe, H., Ohnuki, T., Yanase, N., Sato, T., Kimura, H., Sekine, K., Edis, R., Koppi, A. J., Klessa, D. A., Conoley, C., Nagano, T., Nakashima, S., and Ewing, R. C., 1992, Weathering and its effects on uranium redistribution: Alligator Rivers Analogue Project Final Report, Volume 9, Australian Nuclear Science and Technology Organisation (ANSTO), 138 p.
- OECD/NEA, 1994, The International Alligator Rivers Project—Background and results: Organisation for Economic Co-operation and Development (OECD), Paris, 66 p.
- Payne, T. E., Edis, R., Herczeg, A. L., Sekine, K., Seo, T., Waite, T. D., and Yanase, N., 1992, Groundwater chemistry: Alligator Rivers Analogue Project Final Report, Volume 7, Australian Nuclear Science and Technology Organisation (ANSTO), 185 p.
- Pedersen, C. P., 1987, The geology of the Koongarra deposits, including investigations of contained elements, *in* Koongarra Project Draft Environmental Impact Statement, Appendix 5: Noranda Australia Limited, Melbourne, 97 p.
- Snelling, A. A., 1990, Geological Development of the Koongarra uranium Deposit, *in* Alligator Rivers Analogue Project Progress Report September–November 1990: Australian Nuclear Science and Technology Organisation (ANSTO), p. 7–44.
- Snelling, A. A., 1992, Geological Setting: Alligator Rivers Analogue Project Final Report, Volume 2, Australian Nuclear Science and Technology Organisation (ANSTO), 118 p.
- Sverjensky, D. A., 1992, Geochemical modelling of present-day groundwaters: Alligator Rivers Analogue Project Final Report, Volume 12, Australian Nuclear Science and Technology Organisation (ANSTO), 70 p.
- Townley, L. R., and Barr, A. D., 1992, Two-dimensional regional groundwater flow near Koongarra, *in*: ARAP 3rd Annual Report 1990–1991, Australian Nuclear Science and Technology Organisation (ANSTO), p. 165–193.
- Townley, L. R., Barr, A. D., Braumiller, S., Kawanishi, M., Lever, D. A., Miyakawa, K., Morris, S. T., Raffensberger, J. P., Smoot, J. L., Tanaka, Y., and Trefry, M. G., 1992, Hydrogeological Modelling: Alligator Rivers Analogue Project Final Report, Volume 6, Australian Nuclear Science and Technology Organisation (ANSTO), 133 p.
- van de Weerd, H., Leijnse, A., Hassanizadeh, S. M., and Richardson-van der Poel, M. A., 1994, INTRAVAL Phase 2, Test case 8, Alligator Rivers Natural Analogue—Modelling of uranium transport in the weathered zone at Koongarra (Australia): RIVM Report 715206005, Bilthoven, The Netherlands, 77 p.
- Wyrwoll, K.-H., 1992, Geomorphology and paleoclimatic history: Alligator Rivers Analogue Project Final Report, Volume 3, Australian Nuclear Science and Technology Organisation (ANSTO), 93 p.